Published in final edited form as:
Nat Med. 2006 November ; 12(11): 1301–1309. doi:10.1038/nm1492.

Interleukin-10 determines viral clearance or persistence *in vivo*

David G Brooks[1], **Matthew J. Trifilo**[1], **Kurt H. Edelmann**[1], **Luc Teyton**[2], **Dorian B McGavern**[1,3], and **Michael B A Oldstone**[1,4]

1*Viral Immunobiology Laboratory, Molecular and Integrative Neuroscience Department, The Scripps Research Institute, 10550 North Torrey Pines Road, La Jolla, California 92037, USA.*

2*Department of Immunology, The Scripps Research Institute, 10550 North Torrey Pines Road, La Jolla, California 92037, USA.*

3*The Harold L. Dorris Neurological Research Institute, The Scripps Research Institute, 10550 North Torrey Pines Road, La Jolla, California 92037, USA.*

4*Department of Infectology, The Scripps Research Institute, 10550 North Torrey Pines Road, La Jolla, California 92037, USA.*

Abstract

Persistent viral infections are a major health concern. One obstacle inhibiting the clearance of persistent infections is functional inactivation of antiviral T cells. Although such immunosuppression occurs rapidly after infection, the mechanisms that induce the loss of T-cell activity and promote viral persistence are unknown. Herein we document that persistent viral infection in mice results in a significant upregulation of interleukin (IL)-10 by antigen-presenting cells, leading to impaired T-cell responses. Genetic removal of *Il10* resulted in the maintenance of robust effector T-cell responses, the rapid elimination of virus and the development of antiviral memory T-cell responses. Therapeutic administration of an antibody that blocks the IL-10 receptor restored T-cell function and eliminated viral infection. Thus, we identify a single molecule that directly induces immunosuppression leading to viral persistence and demonstrate that a therapy to neutralize IL-10 results in T-cell recovery and the prevention of viral persistence.

Effective T-cell responses are crucial for the clearance of viral infection. In some instances, however, the immune response is unable to control viral replication, thereby allowing the virus to persist. Concomitant with the transition to persistence, virus-specific $CD4^+$ and $CD8^+$ T cells either are physically deleted or become functionally unresponsive, losing activity and the ability to produce key antiviral and immune stimulatory cytokines[1–9]. The loss of T-cell function occurs during persistent infection by a diverse range of viruses, including HIV and hepatitis B (HBV) and C (HCV) virus infections of humans and lymphocytic choriomeningitis virus (LCMV) infection of rodents[10], indicating that conserved mechanisms of immunosuppression may downregulate T-cell activity. A recent report demonstrated that Programmed Death-1 (PD-1) is critical for sustaining suppression of $CD8^+$ T cells during persistent infection[11]. However, the mechanism(s) that initially induces immunosuppression and leads to the loss of T-cell cytolytic and stimulatory functions is unknown. Here we elucidate a molecule that initiates T-cell inactivation and, consequently, viral persistence.

Correspondence should be addressed to D.G.B. (dbrooks@scripps.edu).

RESULTS

Increased IL-10 production early during persistent viral infection

To determine the mechanism(s) by which viruses induce immunosuppression we used the LCMV model. Infection of mice with the LCMV variant Armstrong (Arm) induces a robust T-cell response that results in viral clearance within 8–10 d (ref. 12). Infection with the LCMV variant Clone 13 (Cl 13), a virus initially derived from LCMV-Arm, generates a persistent infection owing to a single amino acid change in its glycoprotein that enables high-affinity binding to dendritic cells (DCs), accompanied by a marked depletion and inactivation of virus specific T cells[1,13–16]. Arm and Cl 13 share identical epitopes recognized by $CD4^+$ and $CD8^+$ T cells, enabling direct comparison of the virus-specific T-cell responses during acute and persistent infections[17]. We observed 26 times more interleukin (IL)-10 RNA in the spleens of Cl 13–infected mice than in those of Arm-infected mice (Fig. 1a). The known immunosuppressive effect of IL-10 (refs. 18–20) indicated its possible role in potentiating viral persistence.

As IL-10 is primarily produced by mononuclear cells[20], we analyzed *Il10* RNA expression by T cells and antigen-presenting cells (APCs). Although IL-10 protein–producing $CD4^+$ T cells are present *in vivo* until approximately day 5 after Cl 13 infection[1] (Supplementary Fig. 1 online), these cells discontinued IL-10 protein production after functional inactivation (Fig. 1b). Substantial IL-10 protein production by virus-specific $CD8^+$ T cells was also not observed on day 5 (data not shown) or day 9 (Fig. 1b) during Cl 13 infection versus Arm infection. Similar results were observed when total $CD4^+$ and $CD8^+$ T cells were analyzed (data not shown). Only a minimal difference in *Il10* RNA production by T cells was observed in Cl 13–infected compared with Arm-infected mice on day 9 after infection (Fig. 1c). IL-10 protein expression was undetectable in all cell types in uninfected mice (data not shown). Splenic *Il10* RNA levels (Fig. 1d), $CD8^+$ T cell responses and viral titers (data not shown) were equivalent between C57BL/6 wild-type and CD4-deficient mice during Cl 13 infection, clearly indicating that $CD4^+$ T cells are neither the dominant nor a required source of IL-10 leading to viral persistence.

There was a 12-fold increase in the frequency of DCs producing IL-10 protein on day 9 after Cl 13 infection, whereas other APC populations like B cells and macrophages had only minimal increases (Fig. 1b). Early after infection (day 5), DCs from Cl 13–infected mice produced significantly more *Il10* RNA than did those from Arm-infected mice, whereas only a minimal increase occurred in B cells and macrophages (Fig. 1c). By day 9 all APC populations showed more *Il10* RNA expression during Cl 13 infection than during Arm infection, although again DCs exhibited the greatest difference (Fig. 1c). DCs also expressed the highest levels of the IL-10 receptor (IL-10R), CD210, during infection (Supplementary Fig. 2 online), although there was no difference in receptor expression between mice infected with Arm or Cl 13. Sorting myeloid, lymphoid and plasmacytoid DCs indicated that plasmacytoid DCs exhibited similar *Il10* RNA expression during Cl 13 and Arm infections, whereas myeloid and lymphoid DC subsets produced high levels of *Il10* during Cl 13 infection (Fig. 1e). A similar hierarchy of IL-10 protein production was observed in the DC subsets by intracellular cytokine staining directly *ex vivo* (data not shown).

Increased IL-10 production potentiates T-cell inactivation

In C57BL/6 mice, Cl 13 infection resulted in fewer MHC class II and class I tetramer–positive $CD4^+$ and $CD8^+$ T cells, respectively, compared with Arm infection (Fig. 2a,b). Notably, there were significantly more tetramer-positive $CD4^+$ and $CD8^+$ T cells in IL-10–deficient mice infected with Cl 13; in these mice the numbers resembled those observed during Arm infection (Fig. 2a,b). The increased frequency of virus-specific T cells in IL-10–deficient mice was

observed for several immunodominant and subdominant epitopes (Fig. 2c) and corresponded with increased numbers of virus-specific T cells. Lack of *Il10* additionally resulted in the physical preservation of $NP_{396–404}$-specific $CD8^+$ T cell responses that are normally deleted during persistent infection (Fig. 2c).

By day 9 after Cl 13 infection of C57BL/6 mice, $CD4^+$ and $CD8^+$ T cells lose their abilities to make TNF-α and IL-2 in response to viral antigens (Fig. 3a,b). In contrast, $CD4^+$ and $CD8^+$ T cells maintain TNF-α and IL-2 responses in IL-10–deficient mice infected with Cl 13, as they do during during Arm infection (Fig. 3a,b). The preserved functional activity of T cells in IL-10–deficient mice versus C57BL/6 mice infected with Cl 13 was observed for immunodominant and subdominant T-cell responses. During Cl 13 infection in C57BL/6 mice, LCMV-specific cytotoxic T lymphocyte (CTL) activity of spleen cells was rapidly lost, whereas high splenic CTL activity was observed in IL-10–deficient mice (Fig. 3c).

We studied PD-1 levels, the involvement of the Th2 cytokine IL-4 and the role of regulatory T cells. Although PD-1 levels were elevated on virus-specific $CD8^+$ T cells during Cl 13 infection of C57BL/6 mice when compared to Arm infection, they were decreased on virus-specific $CD8^+$ T cells during Cl 13 infection of IL-10–deficient mice (Supplementary Fig. 3 online). PD-1 was expressed at high levels on virus-specific $CD4^+$ T cells throughout all infections regardless of the clearance kinetics (Supplementary Fig. 3), implying that PD-1 interactions may have different effects on $CD4^+$ than $CD8^+$ T cells. The preservation of T-cell function was not observed in IL-4–deficient mice infected with Cl 13 (data not shown), indicating that the retention of T-cell responsiveness observed in IL-10–deficient mice was not a result of a misdirected Th2 response. Lastly, we observed that Foxp3 expression was similar during all infections (Supplementary Fig. 3), arguing against a role for regulatory T cells in Cl 13–infected mice.

Clearance of persistent viral infection in the absence of IL-10

As T cells remained functional, we analyzed whether Cl 13 persisted in the absence of IL-10. After Cl 13 infection of C57BL/6 mice, infectious virus was present in multiple tissue compartments (Fig. 4a). In contrast, Cl 13 was cleared by day 9 after infection in more than 20 mice lacking *Il10*, and infectious virus could not be isolated from the serum, liver or brain (Fig. 4a). Infectious virus could not be isolated on day 42 after Arm infection of C57BL/6 mice or after Cl 13 infection of IL-10–deficient mice, although persisting viral replication was readily observed in Cl 13–infected *Il10*–competent C57BL/6 mice (Fig. 4a). These observations indicate that long-term control of viral replication was achieved in IL-10–deficient mice.

Next we visualized the distribution of virus replication in the spleens of infected mice. Unlike Arm, which replicates primarily in macrophages and is restricted to the red pulp of the spleen, Cl 13 infects high numbers of cells in the splenic white pulp, generating a widespread infection (Fig. 4b).We found that on day 5 after infection, Cl 13 replication in the spleen of IL-10–deficient mice did not resemble Arm infection, but instead was quantitatively and spatially similar to replication seen during Cl 13 infection of C57BL/6 mice (Fig. 4b). Viral titers were similar in the serum and liver of Cl 13–infected C57BL/6 and IL-10–deficient mice 5 d after infection (data not shown). On day 9 after infection, Cl 13 was still widely disseminated in the spleens of C57BL/6 mice (Fig. 4c). In contrast, a marked reduction in viral antigen was observed in IL-10–deficient mice, resulting in amounts of virus that were quantitatively similar to the those observed during Arm infection (Fig. 4c). Despite the similar viral titers in Cl 13–infected C57BL/6 and IL-10–deficient mice on day 5 after infection, no increased immunopathology was associated with the rapid viral clearance in IL-10–deficient mice. Concentrations of serum alanine aminotransferase (sALT, a measure of liver pathology) were equivalent during all infections on day 5. However, by day 9 sALT levels in Cl 13–infected

IL-10–deficient mice were similar to those in Arm-infected C57BL/6 mice but were 1.5 logs lower than those in Cl 13–infected C57BL/6 mice (data not shown). The enhanced viral clearance in IL-10–deficient mice was not associated with increased levels of neutralizing antibodies (nAb), which were absent on day 9 after all infections (data not shown). Thus, deletion of *Il10* facilitates sustained T-cell activity.

Acute clearance of Cl 13 facilitates memory T-cell development

Similar numbers of virus-specific $CD4^+$ T cells were observed during Arm and Cl 13 infection in both C57BL/6 and IL-10–deficient mice on day 42 after infection (Fig. 5). Whereas virus-specific $CD4^+$ T cell functional responses were still depressed during Cl 13 infection in C57BL/6 mice, functional suppression was not observed in C57BL/6 mice that had been infected with Arm or in IL-10–deficient mice that had been infected with Cl 13 (Fig. 5c). At the single-cell level, $CD4^+$ T cells from IL-10–deficient mice produced significantly more IL-2 (based on mean fluorescence intensity; $P < 0.03$; Fig. 5c) and TNF-α ($P < 0.03$; data not shown) than cells from Cl 13–infected C57BL/6 mice. Unlike that of $CD4^+$ T cells, the number of virus-specific $CD8^+$ T cells remained lower throughout Cl 13 infection in C57BL/6 mice (Fig. 5b). However, in IL-10–deficient mice the number of virus-specific $CD8^+$ T cells was similar to that observed 42 d after Arm infection. Virus-specific $CD8^+$ T cells in IL-10–deficient mice retained functional capacity well after infection, whereas their counterparts in C57BL/6 mice after Cl 13 infection remained non-responsive (Fig. 5d). Notably, IL-10–deficient mice previously infected with Cl 13 were resistant to re-infection after viral rechallenge (data not shown), indicating the development of competent memory T-cell responses.

Antibody blockade of IL-10 receptor prevents viral persistence

We next determined whether antibody blockade of IL-10 could prevent or control viral replication after the establishment of infection. C57BL/6 mice were infected with Cl 13 and then treated on days 1 and 5 after infection with an IL-10R–blocking antibody (data not shown). In antibody-treated mice, serum viral titers were decreased by over 2 logs by day 9 after infection, and by day 15 after infection no infectious virus was detected in the serum (Fig. 6a) or other organs. IL-10R blockade resulted in increased numbers of virus-specific T cells and sustained T-cell activity (Fig. 6b–d). We further assessed whether administration of IL-10R–blocking antibody beginning on day 12 after initiation of Cl 13 infection (a time after T-cell inactivation and after clearance of Arm infection) would have a quantitative impact on viral replication. Untreated mice maintained high levels of viral replication (Fig. 6e). In contrast, viral titers decreased rapidly after the initial administration of antibody (assessed at day 15 after infection) and continued to decrease with successive treatments (Fig. 6e). One of the four antibody-treated mice completely cleared the virus by day 35 after infection in spite of initially high viral titers (Fig. 6e), an outcome not seen in over 200 Cl 13–infected untreated mice. A similar decrease in viral replication was also observed in the livers of antibody-treated compared to untreated mice (data not shown). IL-10R blockade during persistence further resulted in an increase in the number of virus-specific $CD8^+$ T cells and increased $CD4^+$ and $CD8^+$ T cell functional responsiveness (Fig. 6f).

DISCUSSION

We identified a single molecule that is upregulated during viral infection and directly induces viral persistence. Our studies document that the increased IL-10 production early during Cl 13 infection induces T-cell inactivation and results in viral persistence. Persistent Cl 13 infection is changed into an acute infection by neutralizing IL-10 activity, and therapy correlates with rescue of T-cell responses. Data demonstrating that the sustained T-cell responses prevent viral persistence are supported by the finding that the initial control of Cl 13 infection in IL-10–deficient mice is temporally associated with the establishment of effector T cell responses,

despite the high viral titers before the onset of T-cell activity. That Cl 13 infection in IL-10–deficient mice is not controlled like Arm infection supports two major points. First, it demonstrates the biological significance of T-cell exhaustion and its important role in potentiating viral persistence. Second, the success or failure of the immune response in preventing viral persistence is not dictated by the initial high levels of viral replication *per se*. Rather, an overwhelming infection can be rapidly cleared by maintaining T-cell activity. Elevated levels of IL-10 are observed during HIV, HCV and HBV infections of humans and, as they do in our results, correlate with diminished T-cell activity and the failure to control viral replication[21–27]. *In vitro* neutralization of IL-10 activity in peripheral blood mononuclear cells from HIV- and HCV-infected humans leads to the restoration of activity in non-responsive T cells[28–30]. Thus, it is likely that IL-10–induced immunosuppression is active during these infections and that neutralization of IL-10 may enhance the treatment of these persistent infections. Nonetheless, not all persistent viral infections are associated with increased IL-10 production or are prevented in IL-10–deficient mice[31,32], indicating that the antiviral effect of neutralizing IL-10 activity should be specifically tested for individual viruses.

The lack of PD-1 expression by $CD8^+$ T cells on day 9 in Cl 13–infected IL-10–deficient mice is likely to be due to the rapid control of viral replication in the absence of IL-10, rather than to a specific regulation of PD-1 by IL-10. A previous study[11] showed that PD-1 expression was increased on virus-specific $CD8^+$ T cells on day 6 after both Arm and Cl 13 infection; however, PD-1 expression decreased in Arm-infected mice after viral clearance. Unlike the case in $CD8^+$ T cells, we observed elevated PD-1 expression on $CD4^+$ T cells 9 d after Arm and Cl 13 infection even in IL-10–deficient mice. These data indicate that IL-10 may not directly regulate PD-1, but that instead immunosuppression may be a multistep process in which increased IL-10 initially induces the suppressive environment that prevents viral clearance, thereby leading to sustained PD-1 expression and long-term T-cell inactivation. A similar correlation between PD-1 expression on T cells and viral loads during HIV infection was recently established, and *in vitro* neutralization of PD-1 during HIV infection alleviated $CD8^+$ T cell exhaustion[33,34]. Although blockade of IL-10 or PD-1 has not been analyzed *in vivo* during HIV or HCV infections, it is possible that each treatment separately, or the two in combination, could serve to restore T-cell functions and control or eliminate infection.

Dendritic cells exhibit the most substantial increase in IL-10 production during persistent infection, although other APC populations, particularly B cells, also express higher levels of IL-10 and may contribute to immunosuppression. Increased IL-10 production by APCs is also observed during HIV and HCV infections and has been shown to specifically downregulate T-cell responses[24,26,35–37]. Because IL-10 can induce T-cell unresponsiveness when present during T-cell activation[19], the ongoing interaction of immunosuppressive IL-10–producing APCs with T cells probably leads to the loss of T-cell responsiveness and the failure to prevent viral persistence. Alternatively, IL-10 may directly affect the APC's ability to stimulate T-cell responses by suppressing antigen-presenting capabilities[18,20,35]. It is unclear exactly what triggers the increased IL-10 expression. DCs are the new primary target of LCMV-Cl 13, compared with Arm[14–16], so it is possible that direct infection causes upregulation of IL-10. However, it is possible that, in response to secondary factors triggered by high levels of minimally controlled virus replication, APCs attempt to dampen the immune response and limit immunopathology.

Are there other cellular sources of IL-10 that contribute to immunosuppression? IL-10–producing $CD4^+$ T cells have been reported during HIV and HCV infections, indicating that these cells may have regulatory activity and contribute to immunosuppression[38–41]. Virus-specific $CD4^+$ T cells initially produce IL-10 during Cl 13 infection, suggesting a possible regulatory role. However, our *in vivo* studies do not support an important role for $CD4^+$ T cells in the immunosuppression. First, by day 9 after Cl 13 infection, although virus-specific T-cell

responses remain suppressed, the $CD4^+$ T cells no longer produce IL-10 protein. Second, there is no increase in Foxp3–expressing $CD4^+$ T cells. Third, $CD4^+$ T cells do not have *ex vivo* regulatory activity[1]. Finally, immunosuppression and IL-10 production occur in mice genetically depleted of $CD4^+$ T cells. *Il10* RNA levels, viral titers and $CD8^+$ T cell inactivation are all equal in C57BL/6 and CD4-deficient mice. The failure of $CD8^+$ T cell responses in the CD4-deficient mice is not due to a secondary effect other than IL-10, as $CD4^+$ T cells are not required to initiate an acute $CD8^+$ T cell response in the LCMV model[42–44]. The early IL-10 production by $CD4^+$ T cells, although not essential, may add to the initial immunosuppression. However, the ability to restore function to unresponsive T cells by removal from the antigenic environment suggests that the immunosuppressive agent is actively sustained[45], consistent with the elevated levels of IL-10 production by APCs. The finding that intrahepatic virus-specific $CD8^+$ T cells produce IL-10 during chronic HCV infection indicates that autocrine suppression by IL-10 may also influence the capacity to fight infection[46].

The acute resolution of Cl 13 infection in IL-10–deficient mice led to the development of T-cell memory. Programming of T-cell memory development does not necessarily occur during priming[45], and the initially high level of viral replication observed in IL-10–deficient mice did not inhibit the signals that potentiate memory. The high level of virus did not affect the number or functional quality of memory precursors, and memory T cells in IL-10–deficient mice seemed to develop similarly to those generated during Arm infection. These memory T cells were able to prevent re-infection upon viral challenge. Thus, by averting T-cell exhaustion and preventing viral persistence, it is possible to develop a population of virus-specific memory T cells.

One of the most noteworthy findings in this study is that *in vivo* antibody blockade of the IL-10R completely prevented viral persistence when administered shortly after infection. Early neutralization of IL-10 activity rescued T cell functional responses that prevented persistent infection. Independent findings of IL-10R blockade controlling persistent infection were also found in another study[47]. Thus, we suggest that therapeutic neutralization of IL-10 activity early after HIV or HCV exposure, such as that occuring during needle stick accidents, may be a feasible therapeutic approach. In addition, *in vivo* blockade of the IL-10R after the onset of T-cell inactivation significantly decreased viral replication and increased T-cell responses. Hence, in addition to initiating the loss of T-cell responses, IL-10 also has a sustained role in perpetuating immunosuppression. IL-10R antibody therapy completely cleared infection in one of four mice and significantly lowered viral titers in the other three, suggesting that it may be possible to purge or better control an established persistent viral infection by neutralizing IL-10 activity. The finding that viral replication was not immediately eliminated by IL-10R antibody treatment administered at the persistent phase of infection may be a function of both an already debilitated T-cell response and the implementation of secondary regulatory factors such as PD-1 (ref. 11) that maintain the suppressive environment induced by IL-10. As IL-10R blockade specifically targets a host factor which does not directly interact with the virus, it is unlikely that viral mutation will allow resistance to therapy, which is a major cause of many treatment failures. Thus, future therapeutic strategies that neutralize IL-10 activity may lead to enhanced control or elimination of persistent viral infections in humans.

METHODS

Mice and virus

C57BL/6 mice were from the Rodent Breeding Colony at the Scripps Research Institute. IL-10–deficient, IL-4–deficient and CD4-deficient mice were obtained from The Jackson laboratory. All mice were housed under specific pathogen–free conditions. Mouse handling conformed to the requirements of the National Institutes of Health and The Scripps Research Institute Animal Research Committee. Mice were infected intravenously with 2×10^6 PFU of LCMV-Arm or

LCMV-Cl 13. To test immunologic memory and protection, mice were rechallenged intravenously with 2.5×10^6 PFU of LCMV-Cl 13. Viral stocks were prepared and viral titers were measured as previously described[1,14,47].

Cell isolation

Total splenic DCs ($CD45^+CD3^-NK1.1^-CD11c^+$), myeloid DCs ($CD45^+CD3^-NK1.1^-CD11c^+CD11b^+$), lymphoid DCs ($CD45^+CD3^-NK1.1^-CD11c^+CD8\alpha^+$), plasmacytoid DCs ($CD45^+CD3^-NK1.1^-CD11c^+B220^+$), B cells ($CD45^+CD3^-NK1.1^-CD11c^-CD19^+$) and macrophages ($CD45^+CD3^-NK1.1^-CD11c^-CD11b^+$) were sorted using a FACSVantage fluorescence-activated cell sorter (Becton Dickinson) as previously described[48]. Purities for all populations after sorting were ≥99%.

Quantitative RT-PCR

RNA from spleen cells (splenocytes) or purified cell populations was isolated with the RNeasy extraction kit (Qiagen). RNA expression was normalized by input concentration and amplified using the One-step RT-PCR kit (Qiagen). The Assays-on-Demand *IL-10* expression kit (Applied Biosystems) was used to amplify *Il10* RNA. The RT-PCR reaction did not amplify DNA (data not shown). For RNA quantification, a standard curve was generated by tenfold serial dilutions of splenic RNA (1 μg to 1 pg total RNA, standard curve $r^2 > 0.99$) from Cl 13–infected splenocytes. The fold increase was then determined by dividing the level of *Il10* in each population during Cl 13 infection by the level in same population during Arm infection. Amplifications were performed on an ABI7700 (Applied Biosystems).

RNase protection assay (RPA)

Total RNA was isolated from spleens at 9 d after infection using TRIZOL reagent (Invitrogen). The level of *Il10* RNA transcripts was determined using the mCK1 probe set (Pharmingen).

Intracellular cytokine analysis and flow cytometry

Splenocytes were stimulated for 5 h with 5 μg/ml of the MHC class II–restricted LCMV $GP_{61–80}$ or $NP_{309-328}$ peptide or 2 μg/ml of the MHC class I–restricted LCMV $NP_{396–404}$, $GP_{33–41}$ or $GP_{276–286}$ peptide (all ≥99% pure; Synpep) in the presence of 50 U/ml recombinant murine IL-2 (R&D Systems) and 1 mg/ml brefeldin A (Sigma). Addition of IL-2 to the *ex vivo* stimulation did not alter cytokine production (data not shown). Cells were stained for surface expression of CD4 (clone RM4-5, Pharmingen) and CD8 (clone 53–6.7, Caltag). Cells were fixed, permeabilized and stained with antibodies to TNF-α (clone MP6-XT22), IFN-γ (clone XMG1.2), IL-2 (clone JES6-5H4) or IL-10 (clone JES5-16E3) (Pharmingen). To analyze IL-10 production by APCs, splenocytes were incubated for 4 h in the presence of 1 mg/ml brefeldin A before staining. Incubation in the presence of LCMV $GP_{61–80}$ or $GP_{33–41}$ peptide did not affect IL-10 expression by the APC subsets. Cells were subsequently stained with subset-specific antibodies (see description of cell isolation above) for DCs, B cells and macrophages and IL-10 production was analyzed. Flow cytometric analysis was performed using a Digital LSR II (Becton Dickinson). MHC class I and class II tetramers were produced as previously described[47] and subsequently stained for expression of PD-1 (monoclonal antibody J43), Foxp3 (monoclonal antibody FJK-16s, eBioscience) or IL-10R (monoclonal antibody 1B1.3a, Pharmingen). The absolute number of virus-specific T cells was determined by multiplying the frequency of $tetramer^+$ or IFN-γ^+ cells by the total number of cells in the spleen.

Microscopy and splenic reconstructions

Two-color reconstructions of spleens were performed with an Axiovert S100 immunofluorescence microscope (Zeiss) fitted with an automated *xy* stage, a Axiocam color digital camera and a ×5 objective. To obtain tissues, organs were removed and frozen in OCT and 6-μm frozen sections were cut and stained overnight at 4 °C with a guinea pig antibody to LCMV (1:1,000 dilution). Tissues were washed, incubated at 4 °C for 3 h with a Rhodamine Red-X–conjugated antibody to guinea pig Fab fragment (1:500), rewashed and incubated with 4,6-diamidino-2-phenylindole (DAPI, 1 μg/ml). Two registered images (DAPI and Rhodamine Red-X) were captured for each field on the spleen section, and reconstructions were done with the MosaiX function in the KS300 image analysis software.

^{51}Cr release assays

In vitro ^{51}Cr release assays were performed on day 9 after infection. MC57 target cells were labeled with 1 μg/ml LCMV $GP_{33–41}$ or $NP_{396–404}$ peptides or left unlabeled, and then mixed with splenocytes at a 50:1 effector/target ratio. Samples were performed in triplicate and ^{51}Cr release was measured in the supernatant after 5 h as previously described[14–16].

In vivo IL-10R–specific antibody treatment

Two treatment regiments were initiated. For the first, C57BL/6 mice received intraperitoneally 500 μg per mouse per injection of IL-10R–specific antibody (clone 1B1.3a, Pharmingen) on days 1 and 5 after Cl 13 infection. For the second experiment, C57BL/6 mice received intraperitoneally 250 μg per mouse per injection of the antibody on days 12, 15, 17 and 19 after Cl 13 infection. Treatment with the rat IgG_1 isotype control antibody (clone R3-34, Pharmingen) had no effect on T-cell responses or viral replication.

Statistical analysis

Student's *t*-tests were performed using the SigmaStat 2.0 software (Systat Software Inc.).

Supplementary Material

Refer to Web version on PubMed Central for supplementary material.

ACKNOWLEDGMENTS

We thank H. Lewicki, D. Young and J. Wheatley for technical assistance and F. Chisari for analysis of sALT levels. Independent findings of IL-10R blockade controlling persistent infection were also found by Ejrneas *et al*. (JEM, in press). Our work was supported by NIH training grant AI07244-22 (D.G.B.), NIH grants AI09484, AI45927 (M.B.A.O.), AI062718-01 (D.B.M.), NS048866-01 (D.B.M.) and a Dana Foundation grant (D.B.M.). This is publication number 18209-MIND from the Viral Immunobiology Laboratory, Department of Molecular and Integrative Neuroscience.

COMPETING INTERESTS STATEMENT

The authors declare that they have no competing financial interests.

References

1. Brooks DG, Teyton L, Oldstone MB, McGavern DB. Intrinsic functional dysregulation of CD4 T cells occurs rapidly following persistent viral infection. J. Virol 2005;79:10514–10527. [PubMed: 16051844]
2. Gallimore A, et al. Induction and exhaustion of lymphocytic choriomeningitis virus-specific cytotoxic T lymphocytes visualized using soluble tetrameric major histocom-patibility complex class I-peptide complexes. J. Exp. Med 1998;187:1383–1393. [PubMed: 9565631]

3. Lechner F, et al. Analysis of successful immune responses in persons infected with hepatitis C virus. J. Exp. Med 2000;191:1499–1512. [PubMed: 10790425]
4. Rosenberg ES, et al. Immune control of HIV-1 after early treatment of acute infection. Nature 2000;407:523–526. [PubMed: 11029005]
5. Thimme R, et al. Determinants of viral clearance and persistence during acute hepatitis C virus infection. J. Exp. Med 2001;194:1395–1406. [PubMed: 11714747]
6. Zajac AJ, et al. Viral immune evasion due to persistence of activated T cells without effector function. J. Exp. Med 1998;188:2205–2213. [PubMed: 9858507]
7. Ou R, Zhou S, Huang L, Moskophidis D. Critical role for alpha/beta and gamma interferons in persistence of lymphocytic choriomeningitis virus by clonal exhaustion of cytotoxic T cells. J. Virol 2001;75:8407–8423. [PubMed: 11507186]
8. van der Most RG, et al. Identification of Db- and Kb-restricted subdominant cytotoxic T-cell responses in lymphocytic choriomeningitis virus-infected mice. Virology 1998;240:158–167. [PubMed: 9448700]
9. Wherry EJ, Blattman JN, Murali-Krishna K, van der Most R, Ahmed R. Viral persistence alters CD8 T-cell immunodominance and tissue distribution and results in distinct stages of functional impairment. J. Virol 2003;77:4911–4927. [PubMed: 12663797]
10. Klenerman P, Hill A. T cells and viral persistence: lessons from diverse infections. Nat. Immunol 2005;6:873–879. [PubMed: 16116467]
11. Barber DL, et al. Restoring function in exhausted CD8 T cells during chronic viral infection. Nature 2005;439:682–687. [PubMed: 16382236]
12. Borrow, P.; Oldstone, MB. Lymphocytic choriomeningitis virus. In: Nathanson, N., editor. Viral Pathogenesis. Philadelphia: Lippincott-Raven; 1997. p. 593-627.
13. Ahmed R, Salmi A, Butler LD, Chiller JM, Oldstone MB. Selection of genetic variants of lymphocytic choriomeningitis virus in spleens of persistently infected mice. Role in suppression of cytotoxic T lymphocyte response and viral persistence. J. Exp. Med 1984;160:521–540. [PubMed: 6332167]
14. Borrow P, Evans CF, Oldstone MB. Virus-induced immunosuppression: immune system-mediated destruction of virus-infected dendritic cells results in generalized immune suppression. J. Virol 1995;69:1059–1070. [PubMed: 7815484]
15. Salvato M, Borrow P, Shimomaye E, Oldstone MB. Molecular basis of viral persistence: a single amino acid change in the glycoprotein of lymphocytic choriomeningitis virus is associated with suppression of the antiviral cytotoxic T-lymphocyte response and establishment of persistence. J. Virol 1991;65:1863–1869. [PubMed: 1840619]
16. Sevilla N, et al. Immunosuppression and resultant viral persistence by specific viral targeting of dendritic cells. J. Exp. Med 2000;192:1249–1260. [PubMed: 11067874]
17. Fuller MJ, Khanolkar A, Tebo AE, Zajac AJ. Maintenance, loss, and resurgence of T cell responses during acute, protracted, and chronic viral infections. J. Immunol 2004;172:4204–4214. [PubMed: 15034033]
18. Fiorentino DF, et al. IL-10 acts on the antigen-presenting cell to inhibit cytokine production by Th1 cells. J. Immunol 1991;146:3444–3451. [PubMed: 1827484]
19. Groux H, Bigler M, de Vries JE, Roncarolo MG. Interleukin-10 induces a long-term antigen-specific anergic state in human CD4+ T cells. J. Exp. Med 1996;184:19–29. [PubMed: 8691133]
20. Moore KW, de Waal Malefyt R, Coffman RL, O'Garra A. Interleukin-10 and the interleukin-10 receptor. Annu. Rev. Immunol 2001;19:683–765. [PubMed: 11244051]
21. Clerici M, et al. Human immunodeficiency virus (HIV) phenotype and interleukin-2/interleukin-10 ratio are associated markers of protection and progression in HIV infection. Blood 1996;88:574–579. [PubMed: 8695805]
22. Orsilles MA, Pieri E, Cooke P, Caula C. IL-2 and IL-10 serum levels in HIV-1-infected patients with or without active antiretroviral therapy. APMIS 2006;114:55–60. [PubMed: 16499662]
23. Cacciarelli TV, Martinez OM, Gish RG, Villanueva JC, Krams SM. Immuno-regulatory cytokines in chronic hepatitis C virus infection: pre- and posttreatment with interferon alfa. Hepatology 1996;24:6–9. [PubMed: 8707283]

24. Brady MT, MacDonald AJ, Rowan AG, Mills KH. Hepatitis C virus non-structural protein 4 suppresses Th1 responses by stimulating IL-10 production from monocytes. Eur. J. Immunol 2003;33:3448–3457. [PubMed: 14635055]
25. Dolganiuc A, et al. Hepatitis C virus core and nonstructural protein 3 proteins induce pro- and anti-inflammatory cytokines and inhibit dendritic cell differentiation. J. Immunol 2003;170:5615–5624. [PubMed: 12759441]
26. Marin-Serrano E, Rodriguez-Ramos C, Diaz F, Martin-Herrera L, Giron-Gonzalez JA. Modulation of the anti-inflammatory interleukin 10 and of proapoptotic IL-18 in patients with chronic hepatitis C treated with interferon alpha and ribavirin. J. Viral Hepat 2006;13:230–234. [PubMed: 16611188]
27. Rico MA, et al. Hepatitis B virus-specific T-cell proliferation and cytokine secretion in chronic hepatitis B e antibody-positive patients treated with ribavirin and interferon alpha. Hepatology 2001;33:295–300. [PubMed: 11124848]
28. Clerici M, et al. Role of interleukin-10 in T helper cell dysfunction in asymptomatic individuals infected with the human immunodeficiency virus. J. Clin. Invest 1994;93:768–775. [PubMed: 8113410]
29. Landay AL, et al. In vitro restoration of T cell immune function in human immunodeficiency virus-positive persons: effects of interleukin (IL)-12 and anti-IL-10. J. Infect. Dis 1996;173:1085–1091. [PubMed: 8627058]
30. Rigopoulou EI, Abbott WG, Haigh P, Naoumov NV. Blocking of interleukin-10 receptor–a novel approach to stimulate T-helper cell type 1 responses to hepatitis C virus. Clin. Immunol 2005;117:57–64. [PubMed: 16006191]
31. Lin MT, Hinton DR, Parra B, Stohlman SA, van der Veen RC. The role of IL-10 in mouse hepatitis virus-induced demyelinating encephalomyelitis. Virology 1998;245:270–280. [PubMed: 9636366]
32. Strestik BD, Olbrich AR, Hasenkrug KJ, Dittmer U. The role of IL-5, IL-6 and IL-10 in primary and vaccine-primed immune responses to infection with Friend retrovirus (Murine leukaemia virus). J. Gen. Virol 2001;82:1349–1354. [PubMed: 11369878]
33. Day CL, et al. PD-1 expression on HIV-specific T cells is associated with T-cell exhaustion and disease progression. Nature 2006;443:350–354. [PubMed: 16921384]
34. Trautmann L, et al. Upregulation of PD-1 expression on HIV-specific CD8 + T cells leads to reversible immune dysfunction. Nat. Med. advance online publication. 2006 August 20;
35. Carbonneil C, Donkova-Petrini V, Aouba A, Weiss L. Defective dendritic cell function in HIV-infected patients receiving effective highly active antiretroviral therapy: neutralization of IL-10 production and depletion of $CD4^+CD25^+$ T cells restore high levels of HIV-specific $CD4^+$ T cell responses induced by dendritic cells generated in the presence of IFN-α. J. Immunol 2004;172:7832–7840. [PubMed: 15187167]
36. Granelli-Piperno A, Golebiowska A, Trumpfheller C, Siegal FP, Steinman RM. HIV-1-infected monocyte-derived dendritic cells do not undergo maturation but can elicit IL-10 production and T cell regulation. Proc. Natl. Acad. Sci. USA 2004;101:7669–7674. [PubMed: 15128934]
37. Ji J, Sahu GK, Braciale VL, Cloyd MW. HIV-1 induces IL-10 production in human monocytes via a CD4-independent pathway. Int. Immunol 2005;17:729–736. [PubMed: 15937058]
38. Kinter AL, et al. $CD25^+CD4^+$ regulatory T cells from the peripheral blood of asymptomatic HIV-infected individuals regulate $CD4^+$ and $CD8^+$ HIV-specific T cell immune responses in vitro and are associated with favorable clinical markers of disease status. J. Exp. Med 2004;200:331–343. [PubMed: 15280419]
39. Lechmann M, et al. Decreased frequency of HCV core-specific peripheral blood mononuclear cells with type 1 cytokine secretion in chronic hepatitis C. J. Hepatol 1999;31:971–978. [PubMed: 10604568]
40. Ostrowski MA, et al. Quantitative and qualitative assessment of human immunodeficiency virus type 1 (HIV-1)-specific $CD4^+$ T cell immunity to gag in HIV-1-infected individuals with differential disease progression: reciprocal interferon-γ and interleukin-10 responses. J. Infect. Dis 2001;184:1268–1278. [PubMed: 11679915]
41. Tsai SL, Liaw YF, Chen MH, Huang CY, Kuo GC. Detection of type 2-like T-helper cells in hepatitis C virus infection: implications for hepatitis C virus chronicity. Hepatology 1997;25:449–458. [PubMed: 9021963]

42. Battegay M, et al. Enhanced establishment of a virus carrier state in adult CD4+ T-cell-deficient mice. J. Virol 1994;68:4700–4704. [PubMed: 7911534]

43. Matloubian M, Concepcion RJ, Ahmed R. CD4+ T cells are required to sustain CD8+ cytotoxic T-cell responses during chronic viral infection. J. Virol 1994;68:8056–8063. [PubMed: 7966595]

44. Tishon A, Lewicki H, Rall G, Von Herrath M, Oldstone MB. An essential role for type 1 interferon-γ in terminating persistent viral infection. Virology 1995;212:244–250. [PubMed: 7676639]

45. Brooks DG, McGavern DB, Oldstone MB. Reprogramming of antiviral T cells prevents inactivation and restores T cell activity during persistent viral infection. J. Clin. Invest 2006;116:1675–1685. [PubMed: 16710479]

46. Accapezzato D, et al. Hepatic expansion of a virus-specific regulatory $CD8^+$ T cell population in chronic hepatitis C virus infection. J. Clin. Invest 2004;113:963–972. [PubMed: 15057302]

47. Homann D, Teyton L, Oldstone MB. Differential regulation of antiviral T-cell immunity results in stable $CD8^+$ but declining $CD4^+$ T-cell memory. Nat. Med 2001;7:913–919. [PubMed: 11479623]

48. Zuniga EI, McGavern DB, Pruneda-Paz JL, Teng C, Oldstone MB. Bone marrow plasmacytoid dendritic cells can differentiate into myeloid dendritic cells upon virus infection. Nat. Immunol 2004;5:1227–1234. [PubMed: 15531885]

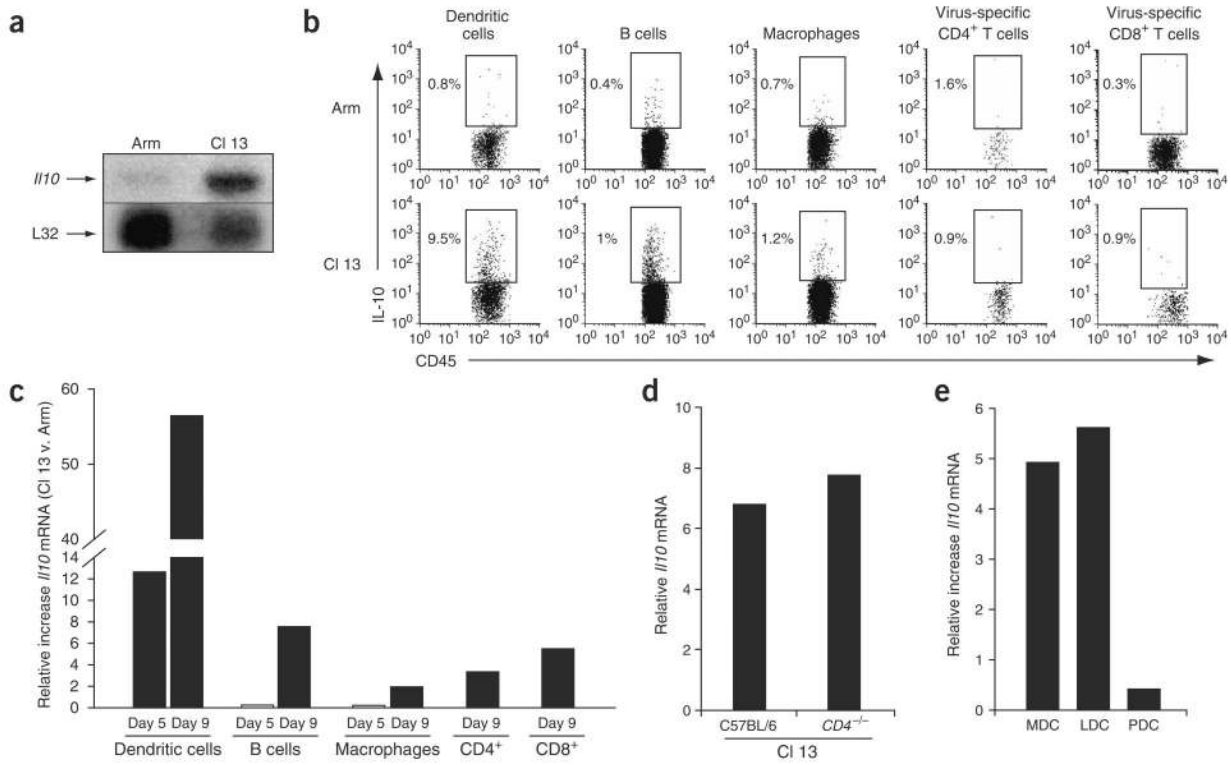

Figure 1.

Increased IL-10 production during persistent viral infection. (**a**) RNA protection assay (RPA) was performed on total splenic RNA on day 9 after Arm or Cl 13 infection. Top and bottom bands show the amounts of *Il10* and the input control L32 RNA, respectively. (**b**) Intracellular cytokine analysis was performed on splenocytes 9 d after Arm or Cl 13 infection. DC, B-cell and macrophage analysis was performed by culture in the absence of CD4-specific or CD8-specific peptides. Virus-specific $CD4^+$ and $CD8^+$ T cells were gated on IFN-γ–producing cells after $GP_{61—80}$ or $GP_{33–41}$ peptide stimulation. For consistency in analysis, all APC and T-cell subsets were gated on CD45 to analyze IL-10 production. The numbers in each plot indicate the frequency of IL-10–producing cells. (**c**) *Il10* RNA in DCs, B cells, macrophages and $CD4^+$ and $CD8^+$ T cells was analyzed by quantitative RT-PCR on days 5 and 9 after Arm or Cl 13 infection. *Il10* RNA production by $CD4^+$ and $CD8^+$ T cells was analyzed on day 9 after infection. Data are represented as the fold increase in *Il10* RNA expression in Cl 13–infected cells versus (v.) Arm-infected cells. Data are from pools of spleens from three or four mice per group and are representative of two to four experiments. (**d**) *Il10* RNA levels were measured by quantitative RT-PCR in total splenocytes on day 9 after Cl 13 infection of C57BL/6 or CD4-deficient ($Cd4^{-/-}$) mice. Data are represented as relative RNA expression compared to a standard curve ($r^2 > 0.99$). Data are from pools of spleens from three or four mice per group and are representative of two experiments. (**e**) *Il10* RNA expression was quantified directly *ex vivo* in myeloid (MDC), lymphoid (LDC) and plasmacytoid (PDC) DCs by quantitative RT-PCR on RNA isolated on day 9 after Arm or Cl 13 infection. Data are represented as the fold increase in *Il10* RNA expression in Cl 13–infected cells versus Arm-infected cells. Data are from pools of spleens from ten mice.

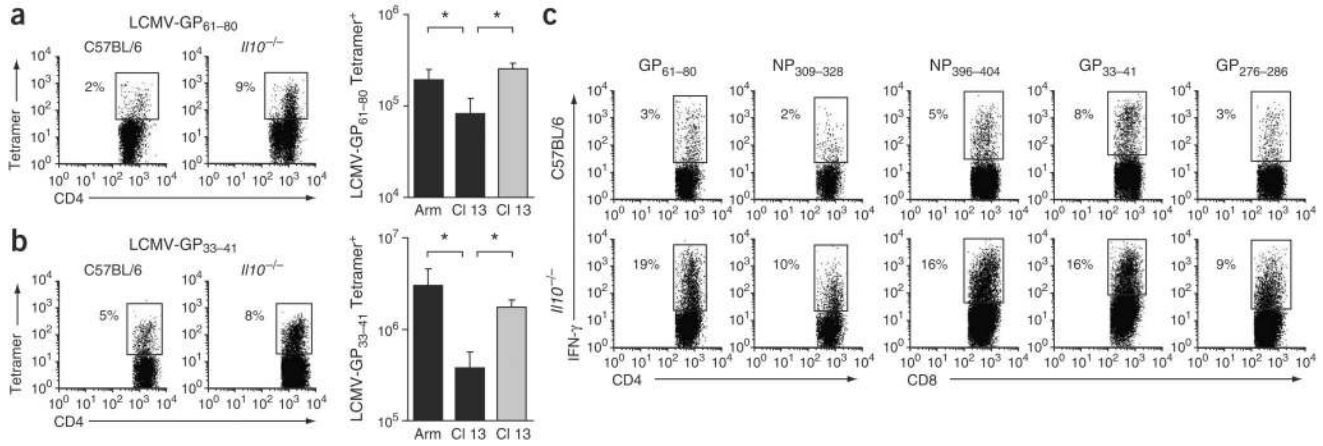

Figure 2.

Increased levels of virus-specific T cells after Cl 13 infection of IL-10–deficient mice. (**a**) Virus-specific $CD4^+$ T cells visualized by $I\text{-}A^b$ $GP_{61—80}$ tetramer staining on day 9 after infection. Flow plots illustrate the frequency of tetramer-positive $CD4^+$ T cells in Cl 13–infected C57BL/6 and *Il10*$^{-/-}$ mice. The bar graph illustrates the average ± 1 s.d. of tetramer-positive cells on day 9 after Arm or Cl 13 infection of C57BL/6 (black) and Cl 13 infection of IL-10–deficient (gray) mice. *$P < 0.03$. (**b**) Virus-specific $CD8^+$ T cells visualized as in **a** with $H\text{-}2D^b$ $GP_{33–41}$ tetramers. Flow plots illustrate tetramer-positive cells in Cl 13–infected C57BL/6 and *Il10*$^{-/-}$ mice. *$P < 0.03$. (**c**) Individual epitope-specific T-cell responses, assessed by *ex vivo* peptide stimulation with the indicated LCMV peptides on day 9 after Cl 13 infection of C57BL/6 or *Il10*$^{-/-}$ mice. Flow plots are gated on $CD4^+$ or $CD8^+$ T cells and numbers illustrate the frequency of IFN-γ^+ $CD4^+$ and $CD8^+$ T cells. Data are representative of four mice per group and two different experiments.

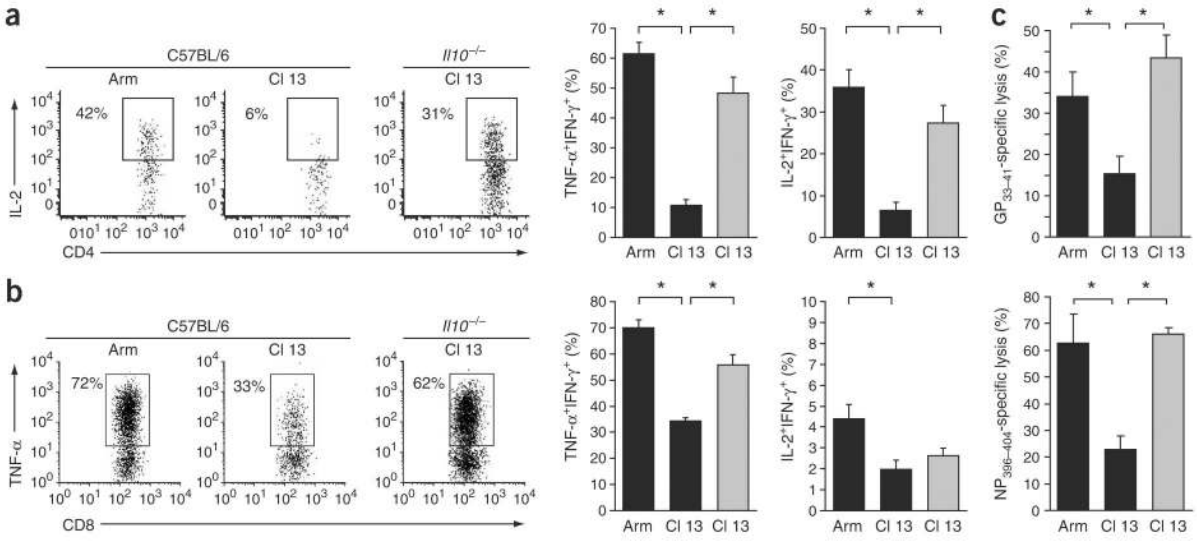

Figure 3.

Sustained effector T cell responses in the absence of IL-10. (**a**) Cytokine production by $CD4^+$ T cells, assessed by *ex vivo* stimulation with $GP_{61—80}$ peptide on day 9 after Arm or Cl 13 infection of C57BL/6 or $Il10^{-/-}$ mice. Flow plots are gated on IFN-γ-producing cells (that is, virus-specific cells) and illustrate the frequency of IL-2–producing, IFN-γ^+ cells. The bar graphs indicate the average ± s.d. of the frequency of TNF-α–producing and IL-2–producing IFN-γ^+ cells from Arm-infected and Cl 13–infected C57BL/6 mice (black) or Cl 13–infected IL-10–deficient mice (gray). *$P < 0.01$. (**b**) Ability of $CD8^+$ T cells to produce effector cytokines after *ex vivo* stimulation with $GP_{33–41}$ peptide, analyzed as in **a**. Flow plots illustrate the average ± s.d. of the frequency of IFN-γ^+ cells that produce TNF-α. *$P < 0.01$. (**c**) ^{51}Cr cytolytic release assay. Bar graphs represent the percent specific lysis of $GP_{33–41}$-labeled or $NP_{396–404}$-labeled target cells by splenocytes from Arm-infected or Cl 13–infected C57BL/6 (black) or Cl 13–infected $Il10^{-/-}$ (gray) mice on day 9 after infection. Values are the average ± s.d. of four mice per group. *$P < 0.01$.

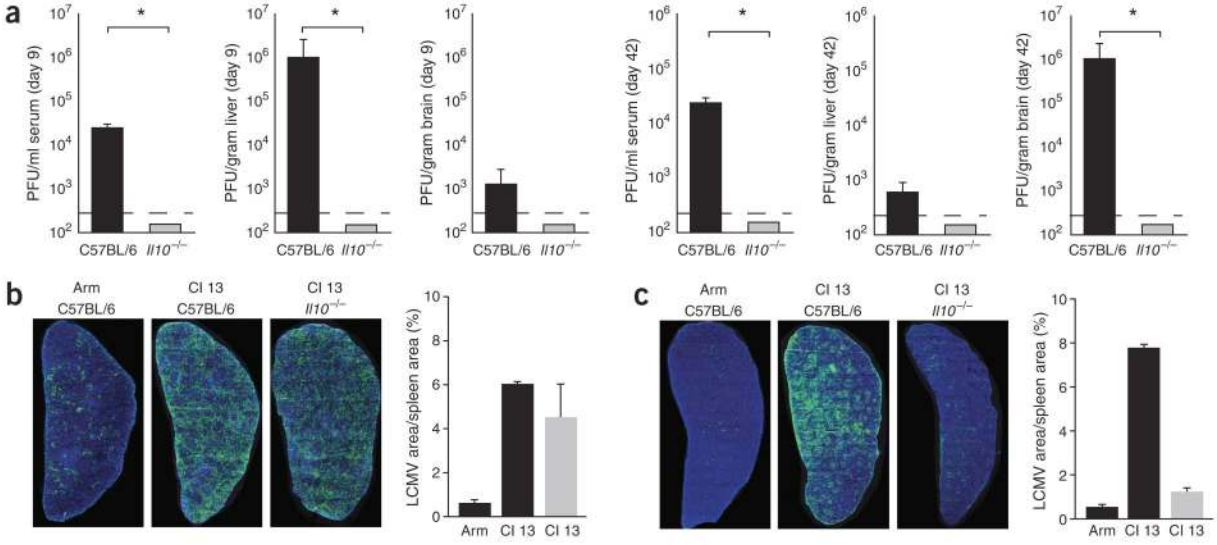

Figure 4.

Increased IL-10 potentiates viral persistence. (**a**) Titers of infectious virus in serum, liver and brain isolated on days 9 and 42 from Cl 13–infected C57BL/6 and IL-10–deficient mice, as determined by plaque assay. Data are expressed as PFU per milliliter of serum or per gram of tissue. The dashed line indicates the lower limit of detection (200 PFU). Each time point represents the average ± s.d. of three or four mice per group. (**b**,**c**) Splenic reconstruction on days 5 (**b**) and 9 (**c**) after Arm infection of C57BL/6 mice, Cl 13 infection of C57BL/6 mice and Cl 13 infection of IL-10–deficient mice. Green, LCMV antigen; blue, DAPI (cell nuclei). Graphs illustrate the area of LCMV antigen per unit tissue (that is, the frequency of infected cells) quantified on days 5 and 9 after the indicated infection using image analysis software. Black bars indicate infection of C57BL/6 mice; gray bars indicate infection of IL-10–deficient mice. Values represent the average ± s.d. of two mice per group.

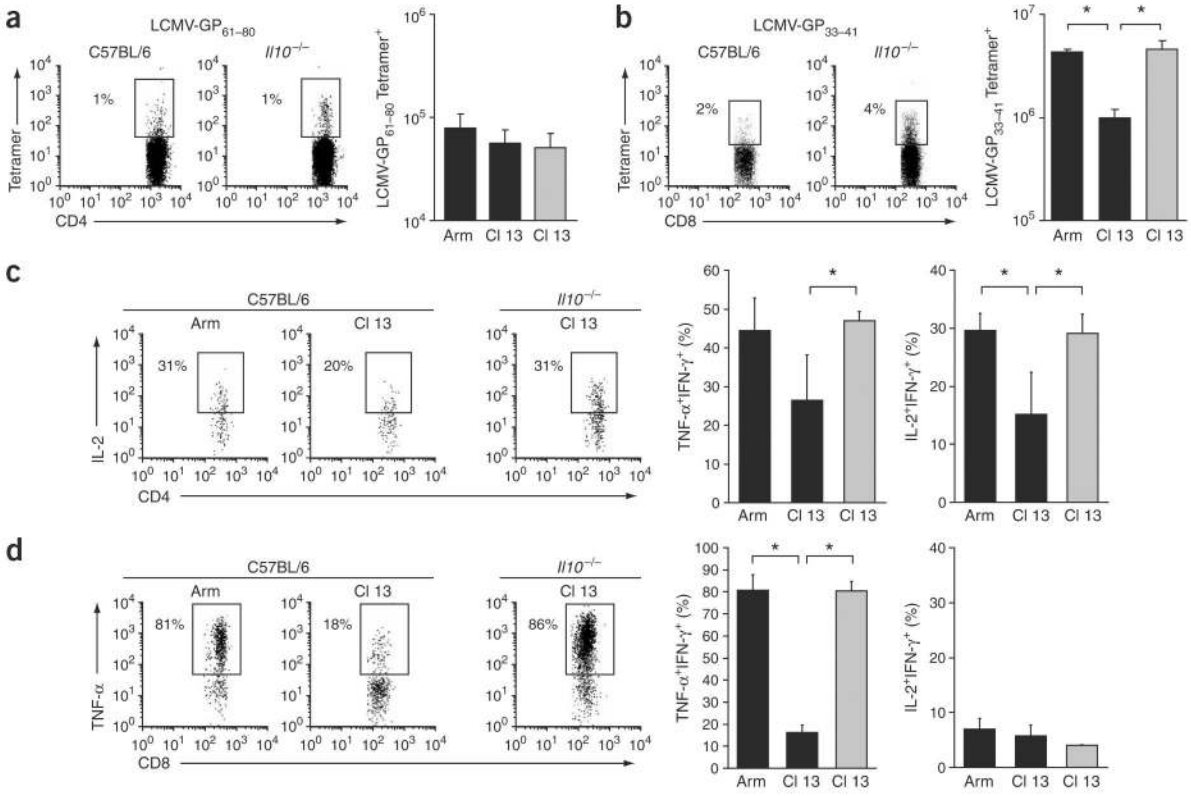

Figure 5.

Rapid clearance of persistent viral infection facilitates memory T-cell development. (**a**) Virus-specific CD4+ T cells visualized by I-A^b $GP_{61—80}$ tetramer staining on day 42 after infection as described in Figure 2a. Flow plots illustrate the frequency of tetramer-positive CD4+ T cells in C57BL/6 (left) and *Il10*$^{-/-}$ (right) mice infected with Cl 13. The bar graph illustrates the number of $GP_{61—80}$ tetramer–positive cells on day 42 after Arm and Cl 13 infection of C57BL/6 mice (black) and Cl 13 infection of *Il10*$^{-/-}$ mice (gray). (**b**) Virus-specific CD8+ T cells visualized as in Figure 2b with H-2D^b $GP_{33–41}$ tetramers; the bar graph shows the number of tetramer-positive cells. *$P < 0.01$. (**c**) Cytokine production by virus-specific CD4+ T cells, assessed on day 42 after Arm or Cl 13 infection of C57BL/6 mice (black) and Cl 13 infection of IL-10–deficient mice (gray bars). Flow plots illustrate the frequency of IL-2 producing, IFN-γ+ cells. Bar graphs, TNF-α and IL-2 production by IFN-γ+ cells. Data are representative of the average ± s.d. of four mice per group. *$P < 0.01$. (**d**) The ability of CD8+ T cells to produce effector cytokines after *ex vivo* stimulation with $GP_{33–41}$ peptide, analyzed as described in Figure 6c. Flow plots illustrate the frequency of TNF-α producing, IFN-γ+ cells. Bar graphs, TNF-α and IL-2 production by IFN-γ+ cells. *$P < 0.01$.

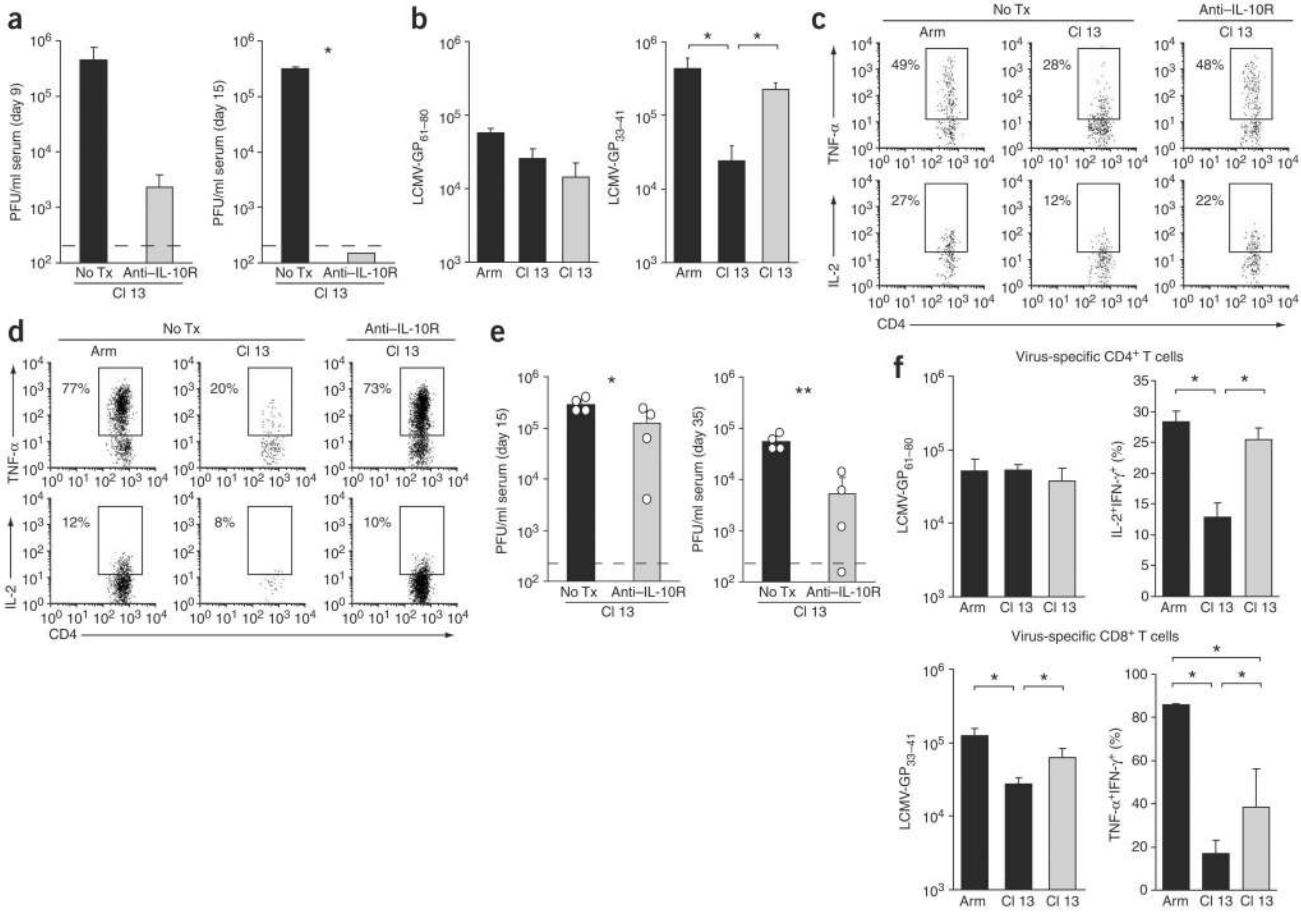

Figure 6.

Treatment with antibody to IL-10R to prevent or treat persistent viral infection. (**a**) C57BL/6 mice were infected with Cl 13 and either left untreated (No Tx) or treated with an IL-10R–blocking antibody on days 1 and 5 after infection. The amount of infectious virus in the serum was quantified on days 9 and 15 after infection. Data are representative of the average ± s.d. of four mice per group. *$P < 0.001$. (**b**) After IL-10R–antibody treatment was initiated on day 1 after infection, virus-specific CD4$^+$ ($GP_{61—80}$) and CD8$^+$ ($GP_{33–41}$) T cells were quantified on day 40 after infection by tetramer staining. The bar graphs show the number of tetramer-positive cells in untreated (black bars) and IL-10R–antibody–treated (gray bars) mice. Data are representative of the average ± s.d. of four mice per group. *$P < 0.01$. (**c**,**d**) Cytokine production by virus-specific CD4$^+$ (**c**) and CD8$^+$ (**d**) T cells was assessed in Arm-infected, Cl 13–infected and IL-10R–antibody–treated Cl 13–infected C57BL/6 mice 40 d after infection. Treatment was initiated on day 1 after infection. Flow plots are gated on IFN-γ$^+$ cells and illustrate the frequency of TNF-α–producing or IL-2–producing, IFN-γ$^+$ cells. Data are representative of four mice per group. (**e**) Serum viral titers in Cl 13–infected C57BL/6 mice either left untreated or treated at 12 d after infection with antibody to IL-10R. The bars in each graph represent the average ± s.d. of four mice per group and the circles indicate the exact value for each mouse in that group. *$P < 0.05$; **$P < 0.005$. (**f**) The number of virus-specific CD4$^+$ ($GP_{61—80}$) and CD8$^+$ ($GP_{33–41}$) T cells was quantified by tetramer staining on day 35 after infection in Arm-infected and Cl 13–infected C57BL/6 (black bars) and IL-10R antibody–treated Cl 13–infected (gray bars) mice. Antibody treatment was initiated 10 d after infection. IL-2 production by virus-specific CD4$^+$ T cells and TNF-α production by virus-specific

$CD8^+$ T cells was assessed by gating on IFN-γ^+ cells and the bar graphs illustrate the frequency of TNF-α or IL-2 producing, IFN-γ^+ cells. Similar data were obtained for TNF-α production by virus-specific $CD4^+$ T cells and IL-2 production by virus-specific $CD8^+$ T cells (data not shown). Values represent the average ± s.d. of four mice per group. $^*P < 0.05$.